

We are IntechOpen, the world's leading publisher of Open Access books Built by scientists, for scientists

6,900

Open access books available

186,000

International authors and editors

200M

Downloads

Our authors are among the

154

Countries delivered to

TOP 1%

most cited scientists

12.2%

Contributors from top 500 universities



WEB OF SCIENCE™

Selection of our books indexed in the Book Citation Index
in Web of Science™ Core Collection (BKCI)

Interested in publishing with us?
Contact book.department@intechopen.com

Numbers displayed above are based on latest data collected.
For more information visit www.intechopen.com



Peripheral Nerve Reconstruction Using Enriched Chitosan Conduits

Shimon Rochkind, Mira M. Mandelbaum-Livnat,
Stefania Raimondo, Michela Morano, Giulia Ronchi,
Nicoletta Viano, Moshe Nissan, Akiva Koren,
Tali Biron, Yifat Bitan, Evgeniy Reider, Mara Almog,
Ofra Ziv-Polat, Abraham Shahar and Stefano Geuna

Additional information is available at the end of the chapter

<http://dx.doi.org/10.5772/intechopen.69882>

Abstract

The repair of peripheral nerve traumatic lesions still represents a major cause of permanent motor and sensory impairment. In case of substance loss, a nerve guide should be used to bridge the proximal with the distal stump of the severed nerve. The effectiveness of hollow nerve guides is limited by the delay of axonal growth due to the absence of a regeneration substrate inside the conduit. To fasten up nerve regeneration, nerve guides should thus be enriched by a luminal filler. In this study, we investigated, in a 12-mm rat sciatic nerve defect experimental model, the effectiveness of chitosan-based conduits of different acetylation filled either with a hyaluronic acid gel (NVR gel) or with a magnetic fibrin hydrogel, in comparison with traditional autografts. Results showed that all types of artificial nerve conduits led to functional recovery not significantly different from autografts. By contrast, morphological and morphometrical analyses showed that the best results among nerve guides were found in medium degree of acetylation (DAII: ~5%) chitosan conduits enriched with the NVR gel.

Keywords: peripheral nerve injury, chitosan guidance conduit, conduit acetylation, hyaluronic acid gel, magnetic fibrin hydrogel

1. Introduction

Chitosan is a biopolymer derived from chitin that can be extracted in large quantities from the shells of the crustaceans. Among the different applications, the use of chitosan

as a scaffold for neural repair is receiving growing interest from the scientific community and, in particular, many experimental studies have shown that chitosan-based conduits provide an effective scaffold for the reconstruction of peripheral nerve defects [1]. Recently, chitosan hollow nerve guides have been approved for clinical use (Reaxon® Nerve Guide) [2].

In spite of these positive results, the early growth of axons along hollow nerve guides is delayed since the conduit's lumen should first be colonized by connective tissue and Schwann cells migrating from the distal nerve stump [3, 4]. To prevent this occurrence, a luminal filler must be used for providing a substrate for early nerve fiber regeneration [5–7]. A number of different materials have been investigated as luminal fillers for nerve guides, including biological or artificial substrates [8–11].

The aim of the present study was to investigate rat sciatic nerve reconstruction with chitosan conduits filled up with two types of substrates which might potentially improve axon regeneration, namely (i) NVR gel and (ii) magnetic fibrin hydrogel.

NVR gel is a gel based on hyaluronic acid (HA), a non-immunogenic biopolymer that has been proposed for various tissue engineering applications [12, 13]. HA is a glycosaminoglycan composed of disaccharide D-glucuronic acid and N-acetyl-D-glucosamine produced by hyaluronan synthases, a membrane-bound enzyme. It is a component of ECM where it modulates cell adhesion, migration, and neuronal sprouting, and it controls tissue homeostasis and absorbs mechanical shock. HA action is related to its molecular weight; a long polymer (>500 kDA) is generally known as high molecular weight HA (HMW HA) and is found predominantly in the brain where it has a structural role and takes part in various biological process like silences inflammation, angiogenesis and neural differentiation [14]. In the peripheral nerves, HA is one of the prominent components of the Bungner band formed during Wallerian degeneration, and the ablation of HA receptors can reduce cell adhesion and migration [15]. Several studies showed that HA has a positive effects on peripheral nerve regeneration [16, 17].

Fibrin hydrogels are natural polymers made by mixing two blood coagulation components, fibrinogen and thrombin, which form a clot upon mixing.

In previous studies, it was demonstrated that appropriate conjugation of thrombin to iron oxide ($\gamma\text{-Fe}_2\text{O}_3$) magnetic nanoparticles preserved the thrombin-clotting activity, stabilized the thrombin against its major inhibitor, antithrombin III, and improved its storage stability [18, 19]. Moreover, these thrombin-conjugated $\gamma\text{-Fe}_2\text{O}_3$ nanoparticles were used to fabricate novel magnetic fibrin hydrogel scaffolds [20].

2. Materials and methods

2.1. Chitosan tube preparation

Chitosan conduits were provided by Medovent GmbH (Mainz, Germany). They were produced under ISO 13485 conditions from chitin tubes made by extrusion process. Distinctive washing

and hydrolysis steps were then carried out to adjust the required low, medium, and high degree of acetylation (DA): (1) DAI tubes (low DA, ~2%); (2) DAII tubes (medium DA, ~5%); and (3) DAIII tubes (high DA, ~20%). Tubes were finally cut and sterilized by electron beam.

2.2. Preparation of NVR gel

NVR gel was prepared by mixing high molecular weight hyaluronic acid (3×10⁶ Da, BTG Polymers, Kiryat Malachi, Israel) and laminin (Sigma, Rehovot, Israel). The NVR gel was then diluted with nutrient medium (composed of 86% Dulbecco's modified Eagle medium-nutrient mixture F-12), 10% heat-denatured fetal calf serum (FCS), 6 g/L D-glucose, 2 nM glutamine, 25 µg/mL gentamycin, and 50 ng/mL IGF-I, all purchased from Biological Industries, Israel, to a final concentration of 0.5%. NVR gel was then injected into the chitosan tubes immediately before surgical implantation.

2.3. Preparation of the magnetic fibrin hydrogel

Magnetic fibrin hydrogel was prepared by mixing 30 µL of bovine fibrinogen (from stock solution of 100 mg/mL, in PBS without Ca²⁺ and Mg²⁺), 460 µL of a culture medium, and 10 µL of a CaCl₂ aqueous solution (from stock solution of 25 mM). To achieve coagulation, thrombin was conjugated to iron oxide nanoparticles [19–21] and added to the gel (50 µL from a stock solution of 100 µg/mL). The final liquid mixture was then injected into the chitosan conduits immediately before surgical implantation.

2.4. Experimental design and surgical technique

All animal experiments were approved by the Institutional Animal Care and Usage Committee (IACUC) and adhered strictly to the Animal Care Guidelines of University Tel Aviv Sourasky Medical Center (number of approval for animal testing 9-3-12). Female Wistar rats were brought to the vivarium 2 weeks prior to the surgery and housed two per cage with a 12-h light/dark cycle, with free access to food and water. The study was conducted on 45 female Wistar rats (weight 200–250 g), using an experimental model for producing a complete peripheral nerve injury with massive nerve defect that has been recently described [22].

General anesthesia was induced with intraperitoneal injection of xylazine (15 mg/kg) and ketamine (50 mg/kg). Surgical procedures were performed using a high magnification microscope. The left sciatic nerve was exposed and separated from biceps femoris and semimembranosus muscles beginning from the area of branches to the glutei and hamstring muscles and distally to the trifurcation into peroneal, tibial, and sural nerves. The sciatic nerve was completely transected at the third femur level using microsurgical scissors and a 6-mm nerve segment was removed. A 14-mm chitosan hollow conduit of different degrees of acetylation (DAI ~2%; DAII ~5%; DAIII ~20%) filled with 0.5% NVR gel was placed between the proximal and the distal parts of the transected nerve for reconstruction, enabling the nerve to enter the conduit 1 mm on each side, while providing a 12-mm gap between the proximal and distal ends. Two 9–0 non-absorbable sutures were used to anchor the conduit to the epineurium at the proximal and distal nerve stumps (**Figure 1**).

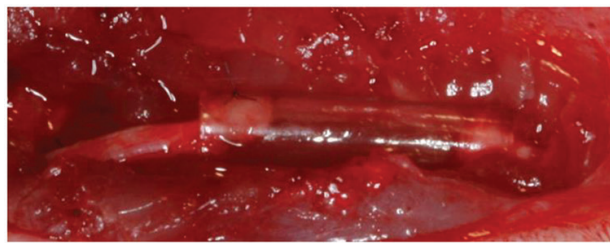


Figure 1. In vivo image of sciatic nerve reconstruction using chitosan-based scaffold immediately after its implantation.

Only one experimental group was used for testing magnetic fibrin hydrogel injected inside DAI tubes.

Autologous nerve graft reconstruction was adopted as control. The left sciatic nerve was exposed as described above and then sharply incised with microscissors at the femur level below the superior gluteal nerve and above the division of the sciatic nerve to the tibial nerve and the peroneal nerve. A nerve segment of 12 mm was harvested, turned upside down, and immediately replaced to bridge the nerve gap using 2–3 non-absorbable 10-0 sutures for each stump. Coaptation of nerve fascicles was carried out to preserve all the fascicles within the epineural sac. The muscular, subcutaneous and skin layers were closed.

Experimental groups can be then summarized as follows: DAI tubes filled with NVR gel ($n = 10$); DAII tubes filled with NVR gel ($n = 10$); DAIII tubes filled with NVR gel ($n = 10$); DAI tubes filled with magnetic fibrin hydrogel ($n = 10$); and autologous nerve grafts ($n = 5$).

2.5. Functional analysis and electrophysiological evaluation

Preoperative evaluation and postoperative follow-up were performed and consisted of motor assessment of the sciatic nerve utilizing sciatic functional index (SFI) (data not shown) and somatosensory evoked potentials (SSEP). SFI and SSEP were tested preoperatively and retested at 90 and 120 days postoperatively.

All assessments were carried out in a blinded manner without disclosure of rat's affiliation to the evaluating team.

SSEP were recorded in both the operated and intact hind limbs using a Dantec™ KEYPONT® PORTABLE. Conductivity of rat sciatic nerve and spinal cord was studied by stimulation of the sciatic nerve at the level of the tarsal joint with simultaneous recording from the skull over the somatosensory cortex in anesthetized rats. Two subcutaneous needle electrodes were inserted under the skin of the scalp with the active electrode over the somatosensory cortex along the midline and reference electrode between the eyes. The ground electrode was placed subcutaneously on the dorsal neck. The sciatic nerve was stimulated by a set of two polarized electrodes placed on the lateral aspect of the tarsal joint. Three hundred

stimulation pulses of 0.2 ms in duration were generated at a rate of 3 Hz. The stimulus intensity was set on 2–5 mA, and a slight twitching of the limb was noted in all rats. The appearance of an evoked potential in at least two consecutive tests as a response to a stimulus was considered positive.

2.6. Morphological and stereological analysis

Nerve samples were collected 120 days after surgery. The complete conduits were harvested together with parts of proximal and distal nerves, and the whole specimens were fixed for 4–6 h at 4°C in 2.5% glutaraldehyde prepared in 0.1 M phosphate buffer (pH 7.4). A postfixation was then performed using 2% osmium tetroxide for 2 h, followed by dehydration in ethanol from 30 to 100%. After two washings with propylene oxide of 7 min each, samples were left for an hour in a mixture of propylene oxide and Glauerts' mixture of resins (50% Araldite HY964, 50% Araldite M, and 0.5% dibutylphthalate) mixed in equal parts. Then, samples were immersed in Glauerts' mixture of resins and left overnight. A second immersion with Glauerts' mixture of resin was then performed, leaving samples at 37°C for 1 h. Samples were then immersed twice for 30 min in resin with the addition of 2% of accelerator 964 and finally left in resin for three days at 60°C. Resin-embedded nerves were then processed for stereological analysis: transverse sciatic nerve sections were prepared starting from the distal part of the samples. For optical analysis, semi-thin sections (2.5 µm of thickness) were prepared using Ultracut UCT ultramicrotome (Leica Microsystems, Wetzlar, Germany) and stained with 1% toluidine blue.

The stereological analysis [23] was performed on semi-thin transverse nerve section stained with toluidine blue using DFC320 digital camera on DM4000B microscope. A random selected semi-thin section was analyzed for each sample with the help of specific image software (IM50 image manager system, Leica Microsystems). The total cross-sectional area of the nerve was measured. Then, 12–16 fields of the section were randomly selected following a systematic random protocol and proceeded as described previously [24] to measure the following parameters: total number of myelinated fibers, axon diameter and fiber diameter, myelin thickness, and g-ratio. Finally, the correlation between g-ratio and axon diameter of individual fibers was carried out as scatter plot graphs.

2.7. Statistical analysis

Functional and electrophysiological analyses were done using MATLAB software (v.2008b, The MathWorks, Inc.). Non-parametric statistics were used in this study. Hence, all figures are presented with Median ± MAD. Significance levels were calculated using a Mann-Whitney U test and a Wilcoxon signed-rank test. SSEP responses were analyzed as categorical parameters using χ^2 test.

For stereological analysis, one-way ANOVA followed by Bonferroni post hoc test was performed using SPSS Statistic Program. The GraphPad software was used to obtain the regression line

in scatter plot and to test whether slopes are significantly different. Results are reported as a mean \pm standard deviation.

3. Results

3.1. Functional analysis and electrophysiological evaluation

Due to autotomy which often occurs in the operated hind limb [25], the number of rats available for meaningful SFI testing was not sufficient for reliable statistics (data not shown). The group of low acetylation conduit (DAI) filled with NVR gel had the lowest number of autotomies (4 out of 10), while the group of low acetylation (DAI) conduit filled with magnetic fibrin hydrogel had the highest number of autotomies (8 out of 10 rats).

For the electrophysiological evaluation, the SSEP peak-to-peak (P2P) amplitude was calculated. Two consecutive electrophysiological recordings were performed on 38 and 39 rats during 90 and 120 days, respectively. In order to evaluate P2P amplitude in the operated and intact limbs, we calculated the results from each limb separately. No significant differences were found between limbs (data not shown). Rats with P2P measurement in only one of the limbs were ignored in calculations from limb comparison. Regarding the operated limb, no significant differences were observed between all groups after both 90 and 120 days (**Figure 2**).

The P2P values of the intact limb were subtracted from the values of the operated limb in order to evaluate the effectiveness of the various conduits and fillers. A value closer to “0” indicates similar activity in both intact and operated limbs, while a major shift is an indicator of neurological dysfunction. As can be seen in **Figure 3**, all groups evolved with a value close to “0,” and no significant difference among the various acetylation conduits and fillers was detected.

3.2. Morphological and stereological analysis

During harvesting (120 days postoperation), a macroscopic observation was performed in order to evaluate the degradation conditions of the conduit and the presence of nerve filaments inside the conduit reconnecting the two nerve stumps. This qualitative analysis showed that 2 rats out of 9 of DAI-NVR gel group and 6 rats out of 10 of DAIII-NVR gel group showed conduits with sign of degradation. Moreover, 5 rats out of 7 of DAI-magnetic fibrin clot group, 7 rats out of 9 of DAI-NVR gel group, 8 rats out of 10 of DAII-NVR gel group, and 8 rats out of 10 of DAIII-NVR gel group showed macroscopically signs of regeneration. This macroscopic observation was then confirmed after histological analysis.

The morphological evaluation was carried out on regenerated nerves immediately downstream to the conduit, 120 days after nerve repair. Representative high-resolution light microscopy images of transverse semi-thin sections of regenerated sciatic nerves of all experimental groups are shown in **Figure 4**. A good regeneration was observed in most of

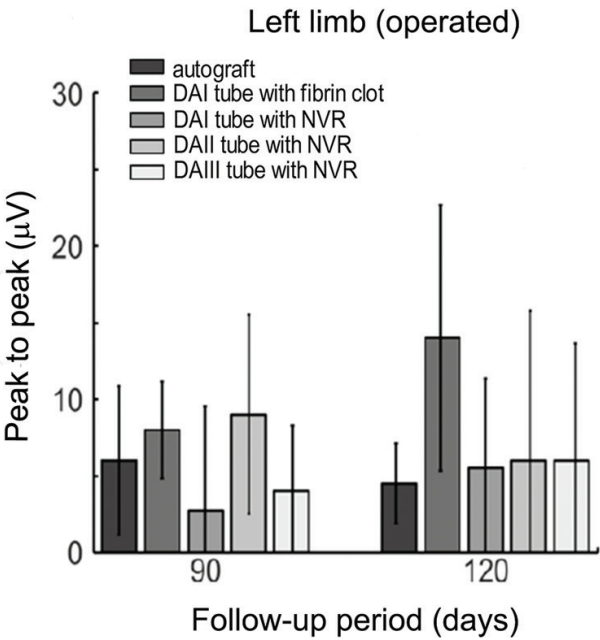


Figure 2. Somatosensory evoked potentials (SSEP) peak-to-peak (P2P) amplitude in operated limbs in various treatments during 90 and 120 days postoperatively. Values are presented with median \pm MAD.

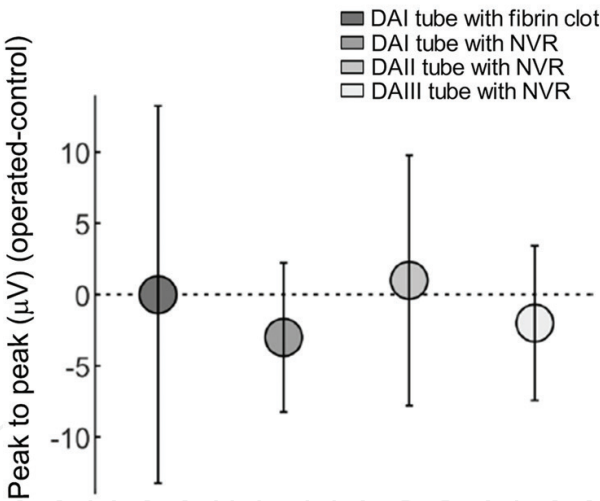


Figure 3. Evaluation of the effectiveness of various acetylation conduits and fillers. The P2P values of the intact limb were subtracted from the values of the operated limb.

the samples for each experimental group: autologous nerve graft (**Figure 4A**); DAI-magnetic fibrin clot (**Figure 4B**); DAI-NVR gel (**Figure 4C**); DAII-NVR gel (**Figure 4D**); DAIII-NVR gel (**Figure 4E**).

Semi-thin sections were also used to perform stereological analysis for the evaluation of the number of myelinated fibers, the axon and fiber size, and the myelin thickness.

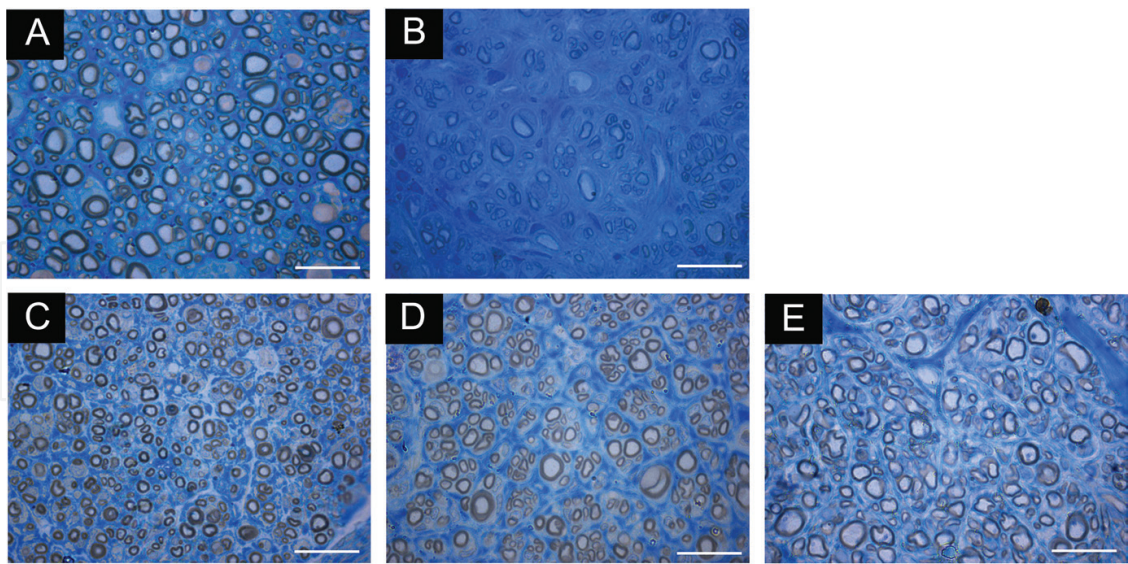


Figure 4. Representative semi-thin sections of the distal part of a sciatic nerve repaired with (A) autologous nerve graft; (B) low acetylation (DAI) conduit filled with magnetic fibrin clot; (C) low acetylation conduit (DAI) filled with NVR gel; (D) medium acetylation (DAII) conduit filled with NVR gel; (E) high acetylation (DAIII) conduit filled with NVR gel. A good regeneration after nerve repair is detectable in all groups. Scale bar: 20 μm .

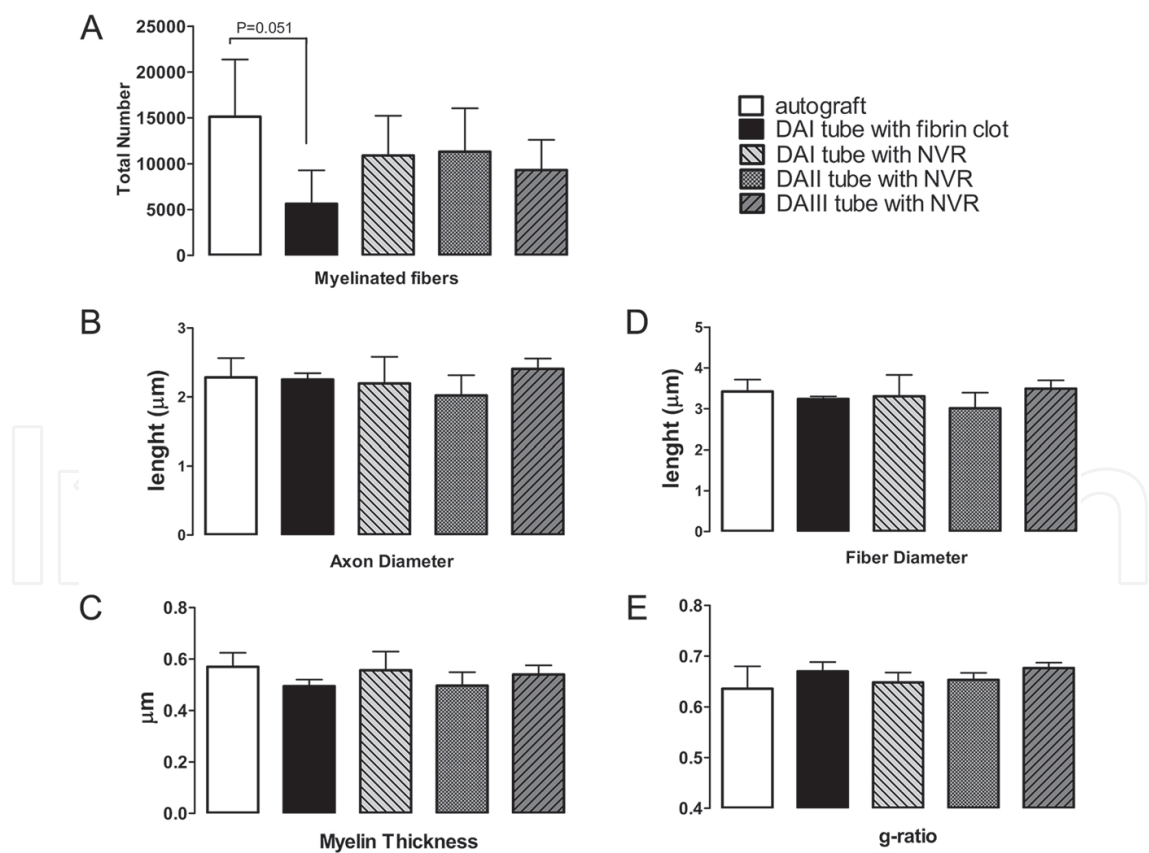


Figure 5. The graphs show the results of stereological analysis on semi-thin sections of the distal part of regenerated nerves. The number of myelinated fibers (A), axon diameter (B), the myelin thickness (C), the fiber diameter (D), and the g-ratio (E) were evaluated 120 days after surgery. All data are presented as means \pm SD; statistical analysis: one-way ANOVA with post hoc Bonferroni test.

As we can observe from the graph (**Figure 5A**), the total number of myelinated fibers in DAI magnetic fibrin clot group is about two-thirds smaller than the autograft group ($p = 0.05$). Moreover, the number of myelinated fibers in all NVR gel groups is similar to each other and about one-third reduced compared to the autograft group. Although the differences are evident, they can only be interpreted as a statistical trend of $p < 0.1$ due to the high standard deviation (that is probably due to the high variability in the regeneration success observed for all-gel-filled conduits).

Axon and fiber diameter, myelin thickness, and g-ratio are not statistically different among all groups (**Figure 5B–E**).

Scatter plot graphs in **Figure 6** represent the correlation between g-ratio and axon diameter of individual fibers. All groups are compared to the autograft, considered as control. Data show that in DAI-magnetic fibrin clot, DAI-NVR gel, and DAIII-NVR gel group, the slope of the regression line is significantly different from the autograft (**Figure 6A, B, D**). Contrary, there is no difference between autograft and DAII-NVR gel group (**Figure 6C**) since the slope of the two regression lines is not significant different.

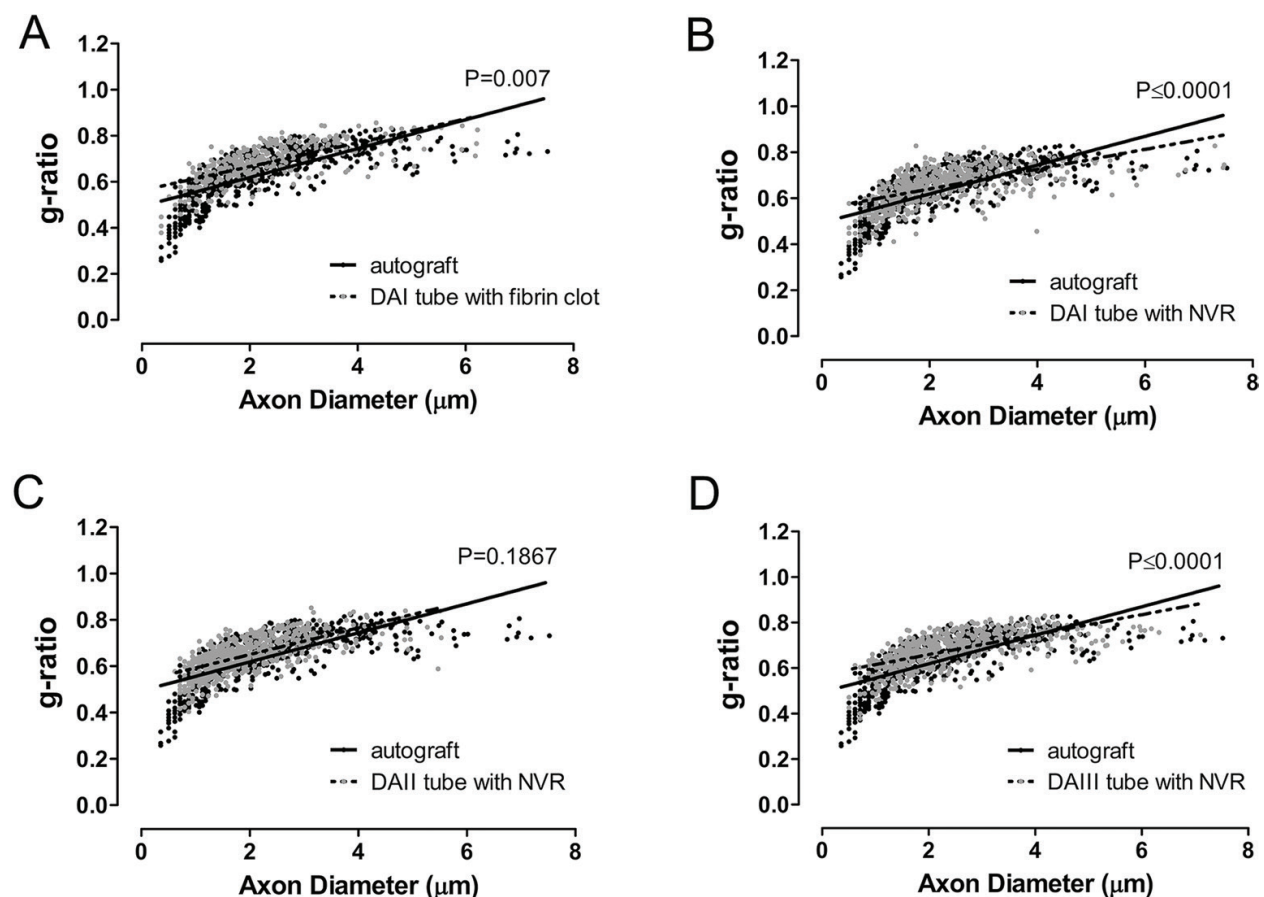


Figure 6. Scatter plot graphs display g-ratio (y-axis) in relation to axon diameter (x-axis) of individual fiber. More than 250 myelinated axons were considered for each group. All the experimental groups are compared to autograft. The slope of linear regression for (A) DAI conduit filled with magnetic fibrin clot, (B) DAI conduit filled with NVR gel, and (D) DAIII conduit filled with NVR gel is significantly different from the autograft. On the contrary, there are no significant differences between autograft and the group DAII conduit filled with NVR gel (C). The statistical analysis was performed using Prism Program, comparing the slope of the linear regression.

4. Discussion

Peripheral nerves are very often subjected to traumatic lesions both because of accidents (e.g., at work, on the road, and at home) and also because of iatrogenic damage (e.g., oncologic surgical excisions) [26, 27]. When the lesion causes substance loss, the two nerve stumps must be connected by a nerve guide in order to allow regenerating axons to bridge the gap [28, 29]. The nerve guide can be represented by an autologous nerve segment (traditional autograft), e.g., from the sural nerve or by a non-nervous conduit [5, 30]. Along the last years, an increasing number of papers describing innovative bio-artificial nerve guides has been published [7]. In general, nerve guides are composed of two main components: a tubular scaffold which can be sutured (or glued) to the nerve stumps and a luminal filler which provides the substrate for cell migration and axon regeneration inside the conduit.

In this study, we selected the chitosan as the biomaterial of choice for fashioning the nerve conduit based on the previous *in vitro* and *in vivo* experimental evidences. *In vitro*, it has been shown that chitosan membranes are a suitable substrate for survival and orientation of Schwann cell growth as well as survival and differentiation of neuronal cells [31, 32]. *In vivo*, studies showed that chitosan tubes can efficiently bridge peripheral nerve defects [33–36].

On the other hand, two types of luminal filler have been investigated in this study: (i) NVR gel and (ii) magnetic fibrin hydrogel.

The selection of NVR gel as a potentially bioactive luminal filler has been based on a number of studies that have proposed his employment for various tissue engineering applications [12, 13]. In peripheral nerves, HA has positive effects on peripheral nerve regeneration modulating glial cell adhesion and migration and neuronal sprouting [15–17]. Yet, topical application of HA is able to reduce the scar formation and create a more favorable environment for nerve regeneration [37, 38].

The results of this study, which compared HA gel enrichment of three different types of chitosan conduits with traditional autografts, showed no significant inter-group differences in the electrophysiological functional outcome and with respect to all histomorphometrical predictors of axon regeneration. By contrast, g-ratio and axon diameter correlation plots (a strong predictor of nerve fiber maturation) showed significant differences between autograft and all groups of conduits except for NVR gel-enriched medium degree of acetylation (DAII). The better performance of DAII (w5%) conduits is in line with a previous report which compared chitosan hollow conduits with different degrees of acetylation in the rat sciatic nerve model [35] and might be explained with the need of a medium-degree degradation time (several months). In fact, the degree of acetylation is directly related to the degradation velocity of the biomaterial, resulting in too slow degradation (more than 1 year) under low acetylation conditions and too fast degradation (several weeks) under high acetylation conditions [35].

As regards the choice of magnetic fibrin hydrogel, the second potentially bioactive luminal filler investigated in this study, this has been based on its previous successful use for tissue engineering applications in various tissues and organs [39–43]. Fibrin hydrogels combine some important advantages such as inherent flexibility, soft, high seeding efficiency, and they

cast easily into three-dimensional shapes, can be injected directly into the site of an injury, and contain cell-binding sites which enhance cell adhesion [44, 45].

In this study, thrombin-conjugated γ -Fe₂O₃ nanoparticles were used to fabricate the magnetic fibrin hydrogel in order to enrich low acetylation (DAI) chitosan conduits. The selection of DAI conduits instead of DAII conduits, which showed a better performance in other experiments (35), was due to the fact that, when these experiments started, full data on the comparison among different acetylation chitosan scaffolds were not available yet.

Results of the electrophysiological assessment showed that no significant difference in functional recovery can be detected between magnetic fibrin hydrogel-enriched DAI conduits, NVR gel-enriched DAI conduits and traditional autografts. By contrast, as regards morphometrical analysis, magnetic fibrin hydrogel-enriched DAI conduits showed significantly less fibers than autograft.

5. Conclusion

Altogether, the results of our study showed that the enrichment of chitosan tubes with both NVR gel and magnetic fibrin hydrogel for the repair of 12 mm long rat sciatic nerve gaps leads to a degree of functional recovery (measured by electrophysiology) not significantly different from traditional autograft. The functional results were not completely matched by the histomorphometric investigation of nerve fibers that showed that best results were found in medium degree (w5%) of acetylation chitosan conduits enriched with the NVR gel. This occurrence, which is not surprising since several studies previously showed that morphological and functional predictors of nerve regeneration are often unrelated [46], must be taken into consideration when translating experimental results to the clinics.

Acknowledgements

This study was supported by the European Community's Seventh Framework Programme (FP7-HEALTH-2011) under grant agreement n° 278612 (BIOHYBRID) and Compagnia di San Paolo (InTheCure Project).

Medical grade chitosan for manufacturing the chitosan films and nerve guides was supplied by Altakitin SA (Lisbon, Portugal). The chitosan materials were supplied by Medovent GmbH (Mainz, Germany). We thank Alex Litvak DVM for technical assistance in animal treatment and care.

Conflict of interest

O. Ziv-Polat and A. Shahar were employees of NVR Research Ltd., while the experiments were conducted, that owns the patent of the NVR gel used in this study.

Author details

Shimon Rochkind¹, Mira M. Mandelbaum-Livnat¹, Stefania Raimondo^{2*}, Michela Morano², Giulia Ronchi², Nicoletta Viano², Moshe Nissan¹, Akiva Koren¹, Tali Biron¹, Yifat Bitan¹, Evgeniy Reider¹, Mara Almog¹, Ofra Ziv-Polat³, Abraham Shahr³ and Stefano Geuna²

*Address all correspondence to: stefania.raimondo@unito.it

1 Division of Peripheral Nerve Reconstruction, Department of Neurosurgery, Research Center for Nerve Reconstruction, Tel Aviv Sourasky Medical Center, Tel Aviv University, Israel

2 Department of Clinical and Biological Sciences, Neuroscience Institute Cavalieri Ottolenghi, University of Turin, Italy

3 NVR Research Ltd., Ness Ziona, Israel

References

- [1] Gnani S, Barwig C, Freier T, Haastert-Talini K, Grothe C, Geuna S. The use of chitosan-based scaffolds to enhance regeneration in the nervous system. *International Review of Neurobiology*. 2013;**109**:1-62
- [2] Neubrech F, Heider S, Harhaus L, Bickert B, Kneser U, Kremer T. Chitosan nerve tube for primary repair of traumatic sensory nerve lesions of the hand without a gap: Study protocol for a randomized controlled trial. *Trials*. 2016;**17**:48
- [3] Hall SM, Redford EJ, Smith KJ. Tumour necrosis factor- α has few morphological effects within the dorsal columns of the spinal cord, in contrast to its effects in the peripheral nervous system. *Journal of Neuroimmunology*. 2000;**106**(1-2):130-136
- [4] Geuna S, Raimondo S, Ronchi G, Di Scipio F, Tos P, Czaja K, et al. Chapter 3: Histology of the peripheral nerve and changes occurring during nerve regeneration. *International Review of Neurobiology*. 2009;**87**:27-46
- [5] Deumens R, Bozkurt A, Meek MF, Marcus MA, Joosten EA, Weis J, et al. Repairing injured peripheral nerves: Bridging the gap. *Progress in Neurobiology*. 2010;**92**(3):245-276
- [6] Geuna S, Gnani S, Perroteau I, Tos P, Battiston B. Tissue engineering and peripheral nerve reconstruction: An overview. *International Review of Neurobiology*. 2013;**108**:35-57
- [7] Chiono V, Tonda-Turo C. Trends in the design of nerve guidance channels in peripheral nerve tissue engineering. *Progress in Neurobiology*. 2015;**131**:87-104
- [8] Geuna S, Tos P, Battiston B, Guglielmone R, Giacobini-Robecchi MG. Morphological analysis of peripheral nerve regenerated by means of vein grafts filled with fresh skeletal muscle. *Anatomy and Embryology (Berlin)*. 2000;**201**(6):475-482

- [9] Geuna S, Tos P, Battiston B, Giacobini-Robecchi MG. Bridging peripheral nerve defects with muscle-vein combined guides. *Neurological Research*. 2004;**26**(2):139-144
- [10] Tos P, Battiston B, Nicolino S, Raimondo S, Fornaro M, Lee JM, et al. Comparison of fresh and predegenerated muscle-vein-combined guides for the repair of rat median nerve. *Microsurgery*. 2007;**27**(1):48-55
- [11] Sedaghati T, Seifalian AM. Nanotechnology and bio-functionalisation for peripheral nerve regeneration. *Neural Regeneration Research*. 2015;**10**(8):1191-1194
- [12] Collins MN, Birkinshaw C. Hyaluronic acid based scaffolds for tissue engineering—A review. *Carbohydrate Polymers*. 2013;**92**(2):1262-1279
- [13] Moshayedi P, Carmichael ST. Hyaluronan, neural stem cells and tissue reconstruction after acute ischemic stroke. *Biomatter*. 2013;**3**(1)pii: e23863
- [14] Preston M, Sherman LS. Neural stem cell niches: Roles for the hyaluronan-based extracellular matrix. *Frontiers in Bioscience (Scholar Edition)*. 2011;**3**:1165-1179
- [15] Tona A, Perides G, Rahemtulla F, Dahl D. Extracellular matrix in regenerating rat sciatic nerve: A comparative study on the localization of laminin, hyaluronic acid, and chondroitin sulfate proteoglycans, including versican. *Journal of Histochemistry and Cytochemistry*. 1993;**41**(4):593-599
- [16] Adanali G, Verdi M, Tuncel A, Erdogan B, Kargi E. Effects of hyaluronic acid-carboxymethylcellulose membrane on extraneural adhesion formation and peripheral nerve regeneration. *Journal of Reconstructive Microsurgery*. 2003;**19**(1):29-36
- [17] Zor F, Deveci M, Kilic A, Ozdag MF, Kurt B, Sengezer M, et al. Effect of VEGF gene therapy and hyaluronic acid film sheath on peripheral nerve regeneration. *Microsurgery*. 2014;**34**(3):209-216
- [18] Margel S, Sheichat L, Tennenbaum T, inventors. Biological Glues based on Thrombin Conjugated Nanoparticles. Israel: Bar-Ilan University [assignee]; 2009
- [19] Ziv-Polat O, Lublin-Tennenbaum T, Margel S. Synthesis and characterization of thrombin conjugated γ -Fe₂O₃ magnetic nanoparticles for hemostasis. *Advanced Engineering Materials*. 2009;**11**:B251-B260
- [20] Ziv-Polat O, Skaat H, Shahar A, Margel S. Novel magnetic fibrin hydrogel scaffolds containing thrombin and growth factors conjugated iron oxide nanoparticles for tissue engineering. *International Journal of Nanomedicine*. 2012;**7**:1259-1274
- [21] Shahar A, Ziv-Polat O, Margel S, Freier T, editors. *Developing a Customized Tissue-Engineered Implant for Peripheral Nerve Reconstruction: Role of Nanoparticles*. USA: Studium Press LLC; 2015
- [22] Shapira Y, Tolmasov M, Nissan M, Reider E, Koren A, Biron T, et al. Comparison of results between chitosan hollow tube and autologous nerve graft in reconstruction of peripheral nerve defect: An experimental study. *Microsurgery*. 2016;**36**(8):664-671

- [23] Geuna S, Herrera-Rincon C. Update on stereology for light microscopy. *Cell and Tissue Research*. 2015;**360**(1):5-12
- [24] Kaplan S, Geuna S, Ronchi G, Ulkay MB, von Bartheld CS. Calibration of the stereological estimation of the number of myelinated axons in the rat sciatic nerve: A multicenter study. *Journal of Neuroscience Methods*. 2010;**187**(1):90-99
- [25] Geuna S. The sciatic nerve injury model in pre-clinical research. *Journal of Neuroscience Methods*. 2015;**243**:39-46
- [26] Siemionow M, Brzezicki G. Chapter 8: Current techniques and concepts in peripheral nerve repair. *International Review of Neurobiology*. 2009;**87**:141-172
- [27] Geuna S, Tos P, Battiston B. Emerging issues in peripheral nerve repair. *Neural Regeneration Research*. 2012;**7**(29):2267-2272
- [28] Battiston B, Raimondo S, Tos P, Gaidano V, Audisio C, Scevola A, et al. Chapter 11: Tissue engineering of peripheral nerves. *International Review of Neurobiology*. 2009;**87**:227-249
- [29] Tos P, Ronchi G, Geuna S, Battiston B. Future perspectives in nerve repair and regeneration. *International Review of Neurobiology*. 2013;**109**:165-192
- [30] Raimondo S, Fornaro M, Tos P, Battiston B, Giacobini-Robecchi MG, Geuna S. Perspectives in regeneration and tissue engineering of peripheral nerves. *Annals of Anatomy*. 2011;**193**(4):334-340
- [31] Freier T, Koh HS, Kazazian K, Shoichet MS. Controlling cell adhesion and degradation of chitosan films by N-acetylation. *Biomaterials*. 2005;**26**(29):5872-5878
- [32] Simoes MJ, Gartner A, Shirosaki Y, Gil da Costa RM, Cortez PP, Gartner F, et al. In vitro and in vivo chitosan membranes testing for peripheral nerve reconstruction. *Acta Médica Portuguesa*. 2011;**24**(1):43-52
- [33] Amado S, Simoes MJ, Armada da Silva PA, Luis AL, Shirosaki Y, Lopes MA, et al. Use of hybrid chitosan membranes and N1E-115 cells for promoting nerve regeneration in an axonotmesis rat model. *Biomaterials*. 2008;**29**(33):4409-4419
- [34] Ao Q, Fung CK, Tsui AY, Cai S, Zuo HC, Chan YS, et al. The regeneration of transected sciatic nerves of adult rats using chitosan nerve conduits seeded with bone marrow stromal cell-derived Schwann cells. *Biomaterials*. 2011;**32**(3):787-796
- [35] Haastert-Talini K, Geuna S, Dahlin LB, Meyer C, Stenberg L, Freier T, et al. Chitosan tubes of varying degrees of acetylation for bridging peripheral nerve defects. *Biomaterials*. 2013;**34**(38):9886-9904
- [36] Meyer C, Stenberg L, Gonzalez-Perez F, Wrobel S, Ronchi G, Udina E, et al. Chitosan-film enhanced chitosan nerve guides for long-distance regeneration of peripheral nerves. *Biomaterials*. 2016;**76**:33-51
- [37] Park JS, Lee JH, Han CS, Chung DW, Kim GY. Effect of hyaluronic acid-carboxymethyl-cellulose solution on perineural scar formation after sciatic nerve repair in rats. *Clinics in Orthopedic Surgery*. 2011;**3**(4):315-324

- [38] Ozgenel GY. Effects of hyaluronic acid on peripheral nerve scarring and regeneration in rats. *Microsurgery*. 2003;**23**(6):575-581
- [39] Ahmed TA, Dare EV, Hincke M. Fibrin: A versatile scaffold for tissue engineering applications. *Tissue Engineering. Part B, Reviews*. 2008;**14**(2):199-215
- [40] Qian LM, Zhang ZJ, Gong AH, Qin RJ, Sun XL, Cao XD, et al. A novel biosynthetic hybrid scaffold seeded with olfactory ensheathing cells for treatment of spinal cord injuries. *Chinese Medical Journal (England)*. 2009;**122**(17):2032-2040
- [41] Uibo R, Laidmae I, Sawyer ES, Flanagan LA, Georges PC, Winer JP, et al. Soft materials to treat central nervous system injuries: Evaluation of the suitability of non-mammalian fibrin gels. *Biochimica et Biophysica Acta*. 2009;**1793**(5):924-930
- [42] Straley KS, Foo CW, Heilshorn SC. Biomaterial design strategies for the treatment of spinal cord injuries. *Journal of Neurotrauma*. 2010;**27**(1):1-19
- [43] Zuidema JM, Provenza C, Caliando T, Dutz S, Gilbert RJ. Magnetic NGF-releasing PLLA/iron oxide nanoparticles direct extending neurites and preferentially guide neurites along aligned electrospun microfibers. *ACS Chemical Neuroscience*. 2015;**6**(11):1781-1788
- [44] Mosesson MW, Siebenlist KR, Meh DA. The structure and biological features of fibrinogen and fibrin. *Annals of the New York Academy of Sciences*. 2001;**936**:11-30
- [45] Laurens N, Koolwijk P, de Maat MP. Fibrin structure and wound healing. *Journal of Thrombosis and Haemostasis*. 2006;**4**(5):932-939
- [46] Ikeda M, Oka Y. The relationship between nerve conduction velocity and fiber morphology during peripheral nerve regeneration. *Brain and Behavior*. 2012;**2**(4):382-390

IntechOpen

